International Journal of Heat and Mass Transfer 75 (2014) 710–717

Contents lists available at ScienceDirect

International Journal of Heat and Mass Transfer

journal homepage: www.elsevier.com/locate/ijhmt

Capillary flow through rectangular micropillar arrays

R.S. Hale [a,*], R. Ranjan [b], C.H. Hidrovo [c]

[a] McKetta Department of Chemical Engineering, The University of Texas at Austin, 200 E. Dean Keeton St., Austin, TX 78712, USA
[b] United Technologies Research Center, 411 Silver Ln, East Hartford, CT 06108, USA
[c] Department of Mechanical and Industrial Engineering, Northeastern University, 360 Huntington Avenue, Boston, MA 02115, USA

ARTICLE INFO

Article history:
Received 16 January 2014
Received in revised form 4 April 2014
Accepted 7 April 2014
Available online 8 May 2014

Keywords:
Capillary flow
Wicking
Micropillar
Rectangular
Permeability
Heat pipe

ABSTRACT

This work explores capillary flow through micropillar arrays with rectangular pillar arrangements. The effects of these configurations on permeability and capillary pressure are investigated for heat pipe wick applications. The permeability is described in terms of three dimensionless parameters: h/d, l/d, and S/d, where l and S are the edge-to-edge spacings in the x- and y-directions, respectively. The two analytical permeability models considered are Hale et al. (2014) [20] and the Brinkman equation using specifically the permeability derived by Tamayol and Bahrami (2009) [19]. Permeability results from numerical simulations are also presented. The surface energy minimization program called Surface Evolver is used to calculate the capillary pressure within the arrays. Mass flow rates are first derived from a combination of array permeability and capillary pressure, and then used to predict the capillary limit of heat pipes equipped with these wicks. Rectangular arrays exhibited the ability to maintain high capillary pressures even at high porosities, which increased the overall cooling capacity above square arrays. The increase was on the order of 1.5× in the absence of gravity and 5×–7× in the presence of gravity, depending on the exact h/d ratio considered.

1. Introduction

Microscale pillar arrays are rapidly gaining popularity due to their wide range of potential applications. Lab-on-a-chip systems are an intensely explored area and have used pillar arrays for high-performance liquid chromatography [1,2], dielectrophoresis [3], and isolating cancer cells [4,5]. Another area of interest is thermal management [6–10], and this work is specifically interested in the use of micropillar arrays in heat pipes. Heat pipes are cooling devices that utilize passive capillary fluid flow through internal wicking structures in a closed system to remove heat via a phase change process. Heat pipes are often limited by the capillary limit, where the capillary pressure in the internal wick can not overcome the resistance to flow through the wick. Thus, one of the key parameters of interest for heat pipes is the size and design of the wick pores. Small pore radii result in a large driving capillary pressure but decrease permeability. For micropillars to be considered as an effective wicking material, the ability to accurately predict the maximum mass flow rate through pillar arrays based on the pillar design is crucial.

The majority of modeling work has been performed for square and hexagonal arrays. Sangani and Acrivos [11], Drummond and Tahir [12], and Gebart [13] studied the permeability of square and hexagonal cylinder arrays over different porosity regimes. Yazdchi et al. [14] summarized the cylinder array permeability models available at the time and compared them to finite element simulations. Xiao and Wang [15], Byon and Kim [16] used the Brinkman equation for flow through porous media to find square pillar array permeability. Srivastava et al. [17] and Ranjan et al. [18] used numerical simulations to model flow through a square pillar array and derive correlations for the permeability as a function of dimensionless geometric parameters. Tamayol and Bahrami [19] used a cell approach to develop an analytical equation for the permeability of long fibers, not pillars, with independent x- and y-direction fiber spacings. Hale et al. [20] analytically modeled actual pillars as opposed to long cylinders, where once again the x- and y-direction pillar spacings were independent, but they did not thoroughly explore the effects of these rectangular configurations on permeability.

Along with permeability, determining the velocity through a pillar array requires knowledge of the driving pressure. Some microfluidic applications require fluid to move as a liquid propagation front, resulting in capillary pressures that relate to surface energies and dynamic meniscus shapes [15,21,22]. However,

* Corresponding author. Tel.: +1 4053380207.
E-mail address: renee.hale@utexas.edu (R.S. Hale).

http://dx.doi.org/10.1016/j.ijheatmasstransfer.2014.04.016
0017-9310/© 2014 Elsevier Ltd. All rights reserved.

Nomenclature

a	aspect ratio for dimensionless velocity model, h/w_{eff}
A_c	cross-sectional wick area (m^2)
d	pillar diameter (m)
g	acceleration of gravity (m^2/s)
h	pillar height (m)
h_{vap}	heat of vaporization (j/g)
K	pillar array permeability (m)
K^*	dimensionless pillar array permeability, K/d^2
K^*_B	dimensionless pillar array permeability using Brinkman equation
$K^*_{T,cyl}$	dimensionless pillar array permeability using [19]
K_{cyl}	2-D cylinder bank permeability
l	pillar spacing in x-direction, center to center (m)
L_{wick}	macroscopic wick length (m)
P	pressure (Pa)
P_l	liquid pressure (Pa)
P_v	vapor pressure (Pa)
ΔP^*_{cap}	dimensionless capillary pressure, $\Delta P_{cap}/(\sigma/d)$
ΔP^*_{total}	dimensionless total liquid pressure drop in model heat pipe
ΔP_{cap}	capillary pressure across vapor–liquid interface (Pa)
ΔP_{grav}	gravitational pressure drop in heat pipe (Pa)
ΔP_{liquid}	liquid phase pressure drop as liquid travels through pillar array (Pa)
ΔP_{vapor}	vapor phase pressure drop as vapor travels through heat pipe (Pa)
$\dot{Q}$	heat transfer rate (W)
S	pillar spacing in y-direction, center to center (m)
s	pillar spacing in y-direction, edge to edge (m)
U	superificial fluid velocity through array (m/s) followed by cooling capacity:
u	x-velocity (m/s)
U^*	dimensionless superifical velocity
$\bar{u}$	dimensionless x-velocity
$\bar{u}_b$	dimensionless velocity profile with respect to $\bar{z}$ located at edges of unit cell $\bar{y} = 1$ and $\bar{y} = 0$
$\bar{u}_{avg}$	dimensionless superficial velocity through a pillar unit cell
$\bar{u}_{max}$	maximum dimensionless velocity at edges of liquid surface, located at $\bar{x} = 0.5$, $\bar{y} = 0$, and $\bar{y} = 1$
W	macroscopic wick width (m)
w	pillar spacing in x-direction, edge to edge (m)
w_{eff}	effective width available for flow (m)
$\bar{y}$	dimensionless y-position, y/l
$\bar{z}$	dimensionless z-position, z/h
Symbols	
β	wick angle relative to ground
ϵ	porosity
μ	fluid viscosity (Pa s)
ρ	liquid density (kg/m^3)
σ	surface tension (N/m)
θ	liquid–solid contact angle

continuous flow technologies such as heat pipes have capillary pressures that rely primarily on the effects of pillar geometry on meniscus shape [6,18,23]. Since rectangular pillar arrangements will create multiple surface radii of curvature, analytical calculations of the effective radius are often inaccurate to predict the capillary pressure [8]. Therefore, capillary pressures for rectangular pillar spacings have been calculated by the surface energy minimization program called Surface Evolver [24], similar to the methods used by Xiao et al. [22]. This study seeks to optimize the effects of independent pillar spacings on array permeability, capillary pressure, and subsequent superficial velocity.

2. Permeability models

The geometry of the pillar array is defined in Fig. 1, where the pillars are of diameter d, height h, edge-to-edge distance in the y-direction w, and edge-to-edge distance in the x-direction s (Fig. 1). Additionally, we define the center-to-center distances as $l = w + d$ and $S = s + d$. A few recent studies have included the effects of meniscus shape on permeability [15,16,22], but the liquid interface at h was kept flat in this study for simplicity. The porosity of the array is given:

$$\epsilon = 1 - \frac{\pi}{4}\left(\frac{d}{l}\right)\left(\frac{d}{S}\right). \quad (1)$$

If the pressure gradient is constant and applied only in the x-direction, then fluid flow occurs primarily in the x-direction in line with the gradient. The Darcy fluid flow relates superficial velocity U to the pressure gradient by

$$U = -\frac{dP}{dx}\frac{K}{\mu}, \quad (2)$$

where μ is the fluid viscosity and K is the array permeability. Permeability is commonly non-dimensionalized by the pillar diameter, so we define $K^* = K/d^2$. Three separate methods of determining the permeability will be compared: the Brinkman equation using the permeability proposed by Tamayol and Bahrami [19], the analytical solution by Hale et al. [20], and numerical simulations.

2.1. Brinkman equation with cylinder array permeability solution by Tamayol and Bahrami [19]

The Brinkman equation is a modified form of the Navier–Stokes equation that is applicable to porous media flow. The Brinkman equation is a popular method to calculate the permeability through pillar arrays [22,25]. However, it requires knowledge of the 2-D permeability of a cylinder array without a bounding surface (K_{cyl}). This presents a challenge for rectangular geometries, since the majority of researchers have studied only square or hexagonal arrays. The governing equation is

$$\frac{\mu}{\epsilon}\frac{d^2u}{dz^2} - \frac{dP}{dx} - \frac{\mu}{K_{cyl}}u = 0, \quad (3)$$

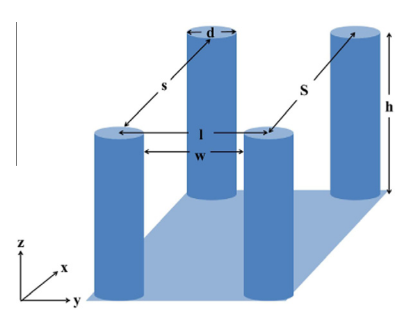

Fig. 1. Micropillar unit cell with geometric parameters. Fluid flow is in the x-direction.